# Supplementary Information

## A versatile single-molecule counting-based platform by generation of fluorescent silver nanoclusters for sensitive detection of multiple nucleic acids

Manshu Peng,[a] Zhuyin Fang,[a] Na Na[a] and Jin Ouyang*[a]

[a]Key Laboratory of Theoretical and Computational Photochemistry, Ministry of Education, College of Chemistry, Beijing Normal University, Beijing 100875, China.

*Corresponding author. E-mail: jinoyang@bnu.edu.cn.

**Table S1** DNA and miRNA sequences used in this study.

| Names | Sequences (5' to 3') |
|---|---|
| FG | TGCCTTTTGGGGACGGATA |
| FR | CCCTAACTCCCC |
| l-MB-21 | TATCCGTCCCCAAAAGGCA*CCCGCTAG*TCAACATCAGTCTG ATAAG*CTAGCGGG* |
| l-MB-let | GGGGAGTTAGGG*CCCGCTGAG*AACTATACAACCTACTAC*CT CAGCGGG* |
| l-MB-let-8b | GGGGAGTTAGGG*CCCGCTGA*AACTATACAACCTACTACC*TC AGCGGG* |
| miR-21 | UAGCUUAUCAGACUGAUGUUGA |
| let-7a | UGAGGUAGUAGGUUGUAUAGUU |
| Assis-21 | CTAGCGGGTGCCTTTTGGGGACGGATA |
| Assis-let | TCAGCGGGCCCTAACTCCCC |
| l-MB-W24 | GGGGAGTTAGGG*AGTTGGAGC*AAAATTGCCTACGCCACCAG *CTCCAACT* |
| l-MB-A24 | TATCCGTCCCCAAAAGGCA*AGTTGGAGC*AAAATTGCCTACG CCATCAG*CTCCAACT* |
| Tw24 | AGTTGGAGCTGGTGGCGTAGGCAA |
| Ta24 | AGTTGGAGCTGATGGCGTAGGCAA |
| Tw18 | AGCTGGTGGCGTAGGCAA |
| Ta18 | AGCTGATGGCGTAGGCAA |

| | |
|---|---|
| Tw15 | TGGTGGCGTAGGCAA |
| Ta15 | TGATGGCGTAGGCAA |
| Tw12 | TGGTGGCGTAGG |
| Ta12 | TGATGGCGTAGG |
| Assis-W24 | GCTCCAACTCCCTAACTCCCC |
| Assis-A24 | GCTCCAACTTGCCTTTTGGGGACGGATA |
| l-MB-W | GGGGAGTTAGGG*CCCGCTGAG*AACCGCCACCAGCTCTAC*CT CAGCGGG* |
| l-MB-A | TATCCGTCCCCAAAAGGCA*CCCGCTAG*TCAACGCCATCAGC TCAAG*CTAGCGGG* |
| Wild (Tw) | GCCTGCTGAAAATGACTGAATATAAACTTGTGGTAGTTGGA GCTGGTGGCGTAGGCAAGAGTGCCTTGACGATACAGCTAA |
| Mutant A (Ta) | GCCTGCTGAAAATGACTGAATATAAACTTGTGGTAGTTGGA GCTGATGGCGTAGGCAAGAGTGCCTTGACGATACAGCTAA |
| l-MB-G-155 | TATCCGTCCCCAAAAGGCA*CCCGCTAG*ACCCCTATCACGAT TAGCA*CTAGCGGG* |
| l-MB-G-7f | TATCCGTCCCCAAAAGGCA*CCCGCTAG*AACTATACAATCTA CTACC*CTAGCGGG* |
| l-MB-R-155 | GGGGAGTTAGGG*CCCGCTGAG*ACCCCTATCACGATTAG*CTC AGCGGG* |
| l-MB-R-7f | GGGGAGTTAGGG*CCCGCTGAG*AACTATACAATCTACTAC*CT CAGCGGG* |
| miR-155 | UUAAUGCUAAUCGUGAUAGGGGU |
| let-7f | UGAGGUAGUAGAUUGUAUAGUU |

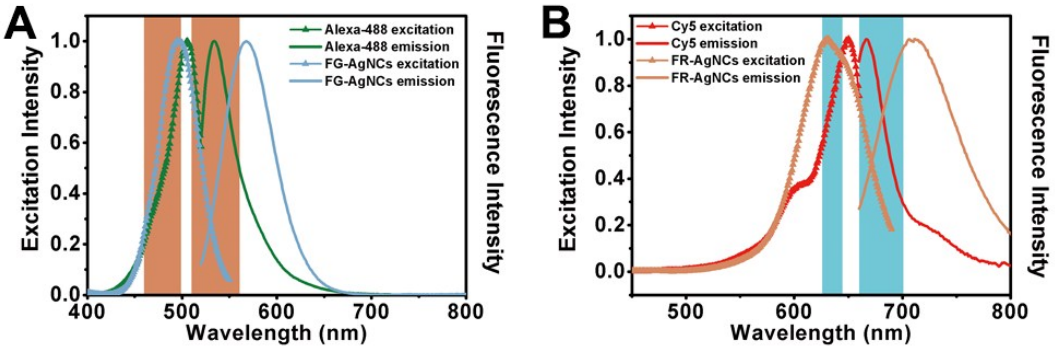


**Fig. S1** Normalized excitation and emission spectra of (A) organic dyes Alexa Fluor 488 and FG-AgNCs and (B) organic dyes Cy5 and FR-AgNCs. The orange areas represent the imaging conditions of Alexa Fluor 488 and FG-AgNCs (The excitation light was passed through a 460-500 nm bandpass filter and the emission was observed through a 510-560 nm barrier filter). The blue areas represent the imaging conditions of Cy5 and FR-AgNCs (The excitation light was passed through a 626-644 nm bandpass filter and the emission was observed through a 659-701 nm barrier filter).

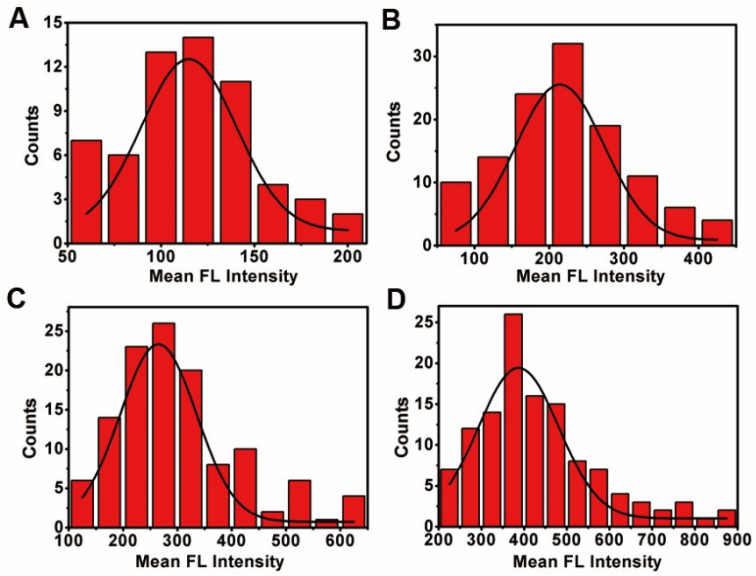


**Fig. S2** Fluorescence intensity distribution of single molecules. (A) FG-Alexa-488, (B) FR-Cy5, (C) FG-AgNCs and (D) FR-AgNCs.

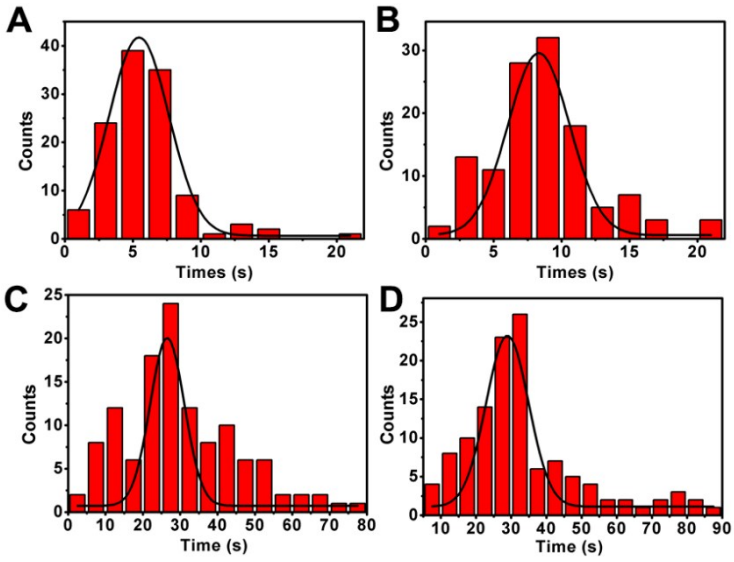


**Fig. S3** The histograms of the emission lasting times of 120 single molecules before bleaching. (A) FG-Alexa-488, (B) FR-Cy5, (C) FG-AgNCs and (D) FR-AgNCs.

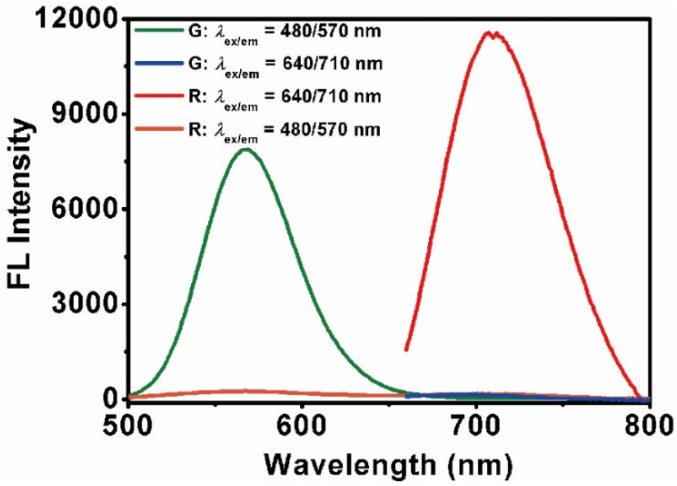


**Fig. S4** The emission spectra of FG-AgNCs and FR-AgNCs.

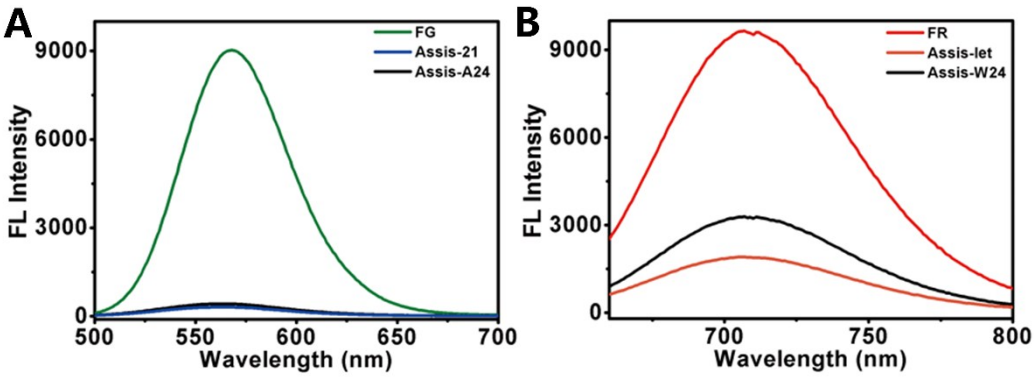


**Fig. S5** (A) The emission spectra of FG-AgNCs, Assis-21-AgNCs and Assis-A24-AgNCs; (B) The emission spectra of FR-AgNCs, Assis-let-AgNCs and Assis-W24-AgNCs.

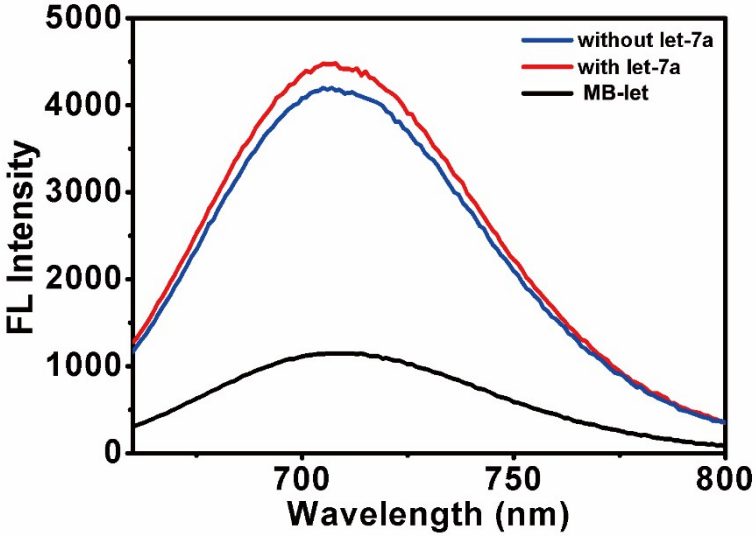


**Fig. S6** The emission spectra of P-let that 8-base pairs were adopted in l-MB-let stem in the absence of targets and assistant DNAs (black line), in the presence of targets (red line) and in the absence of targets (blue line).

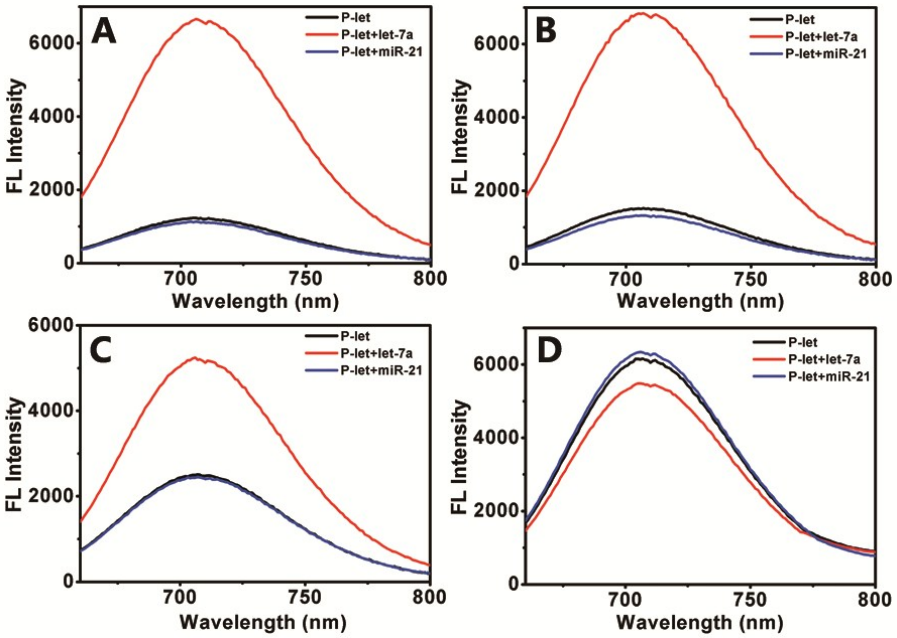


**Fig. S7** The emission spectra of P-let without targets (black line), in the presence of targets let-7a (red line), in the presence of non-targets miR-21 (blue line) with the reaction temperature of DNA strand displacement at (A) 22 °C, (B) 25 °C, (C) 30 °C, (D) 37 °C.

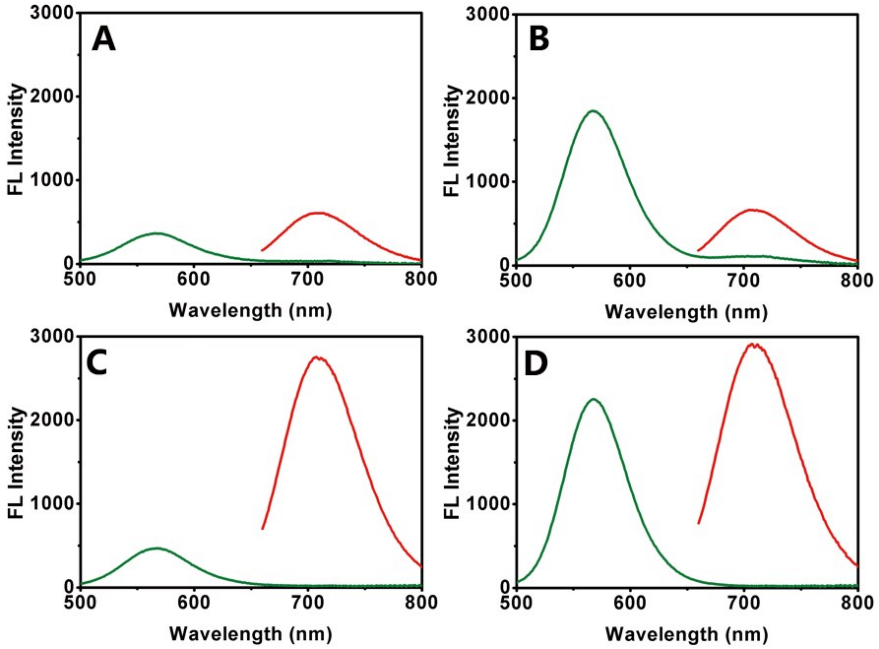


**Fig. S8** Fluorescence spectra of P-21 ($\lambda_{ex}$ = 480 nm) and P-let ($\lambda_{ex}$ = 640 nm) for multiple miRNAs detection (A) in the absence of targets, (B) in the presence of miR-21, (C) in the presence of let-7a, (D) in the presence of miR-21 and let-7a. The concentration of target miRNAs used in the fluorescence detection system is 500 nM.

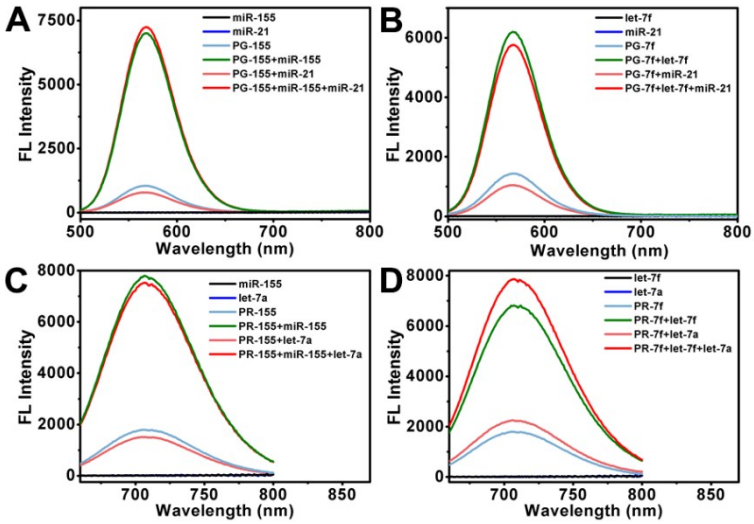


**Fig. S9** Fluorescence emission spectra of targets-stabilized AgNCs, miRNA155 and let-7f miRNA detection systems. (A) PG-155 in the absence of targets, in the presence of targets (miR-155), non-targets (miR-21) and the mixture of miR-155 and miR-21. (B) PG-7f in the absence of targets, in the presence of targets (let-7f), non-targets (miR-21) and the mixture of let-7f and miR-21. (C) PR-155 in the absence of targets, in the presence of targets (miR-155), non-targets (let-7a) and the mixture of miR-155 and let-7a. (D) PR-7f in the absence of targets, in the presence of targets (let-7f), non-targets (let-7a) and the mixture of let-7f and let-7a. PG-155 and PG-7f are the green-emitting AgNCs-MB sensing platforms redesigned for detecting miR-155 and let-7f miRNA, respectively. Likewise, two red-emitting AgNCs-MB sensing platforms were designed and labeled as PR-155 and PR-7f for the detection of miR-155 and let-7f miRNA.

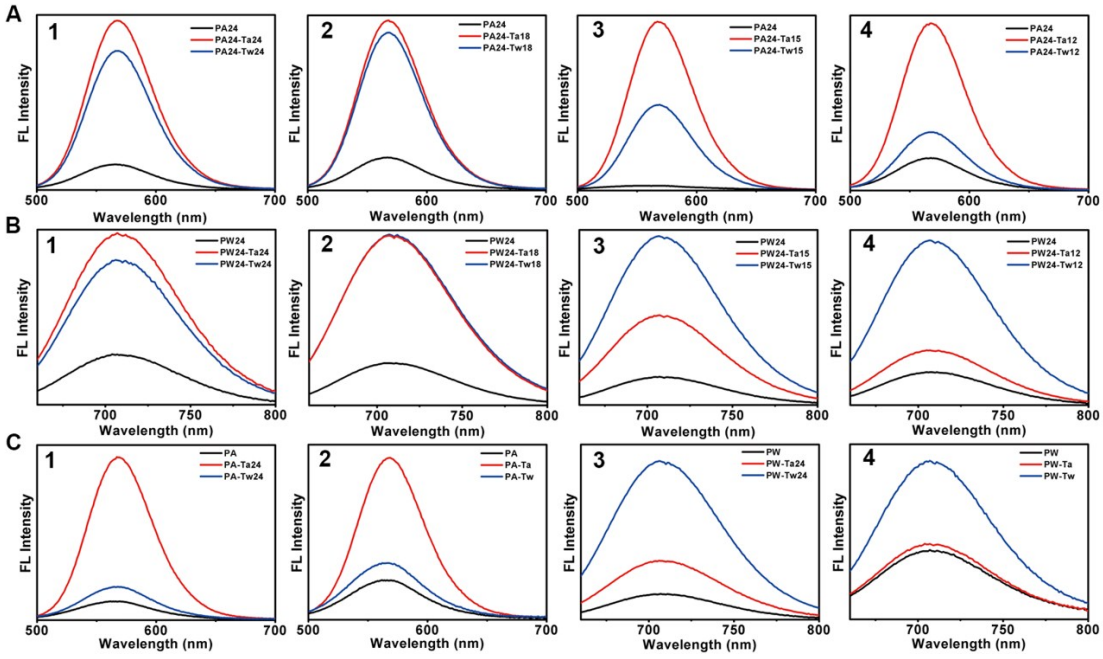


**Fig. S10** Two AgNC-MB sensing platforms (PA24 and PW24), the probes of which

contained 24-base segments complementary to targets, were designed for the detection of mutant A and wild-type sequences, respectively. Fluorescence spectra of (A) PA24 and (B) PW24 in the absence of targets (black lines), in the presence of target segment of wild-type genes (blue lines) and in the presence of target segment of mutant-type genes (red lines). Ta24, Ta18, Ta15 and Ta12 are the 24, 18, 15 and 12-base target segments of mutant-type genes, and Tw24, Tw18, Tw15 and Tw12 are the 24, 18, 15 and 12-base target segments of wild-type genes, respectively. (C) Fluorescence spectra of PA (panel 1 and 2) and PW (Panel 3 and 4) in the absence of targets (black lines), in the presence of target segment of wild-type genes (blue lines) and in the presence of target segment of mutant-type genes (red lines). Ta and Tw are the sequences of KRAS G12D (c.35G>A) mutation and wild-type.

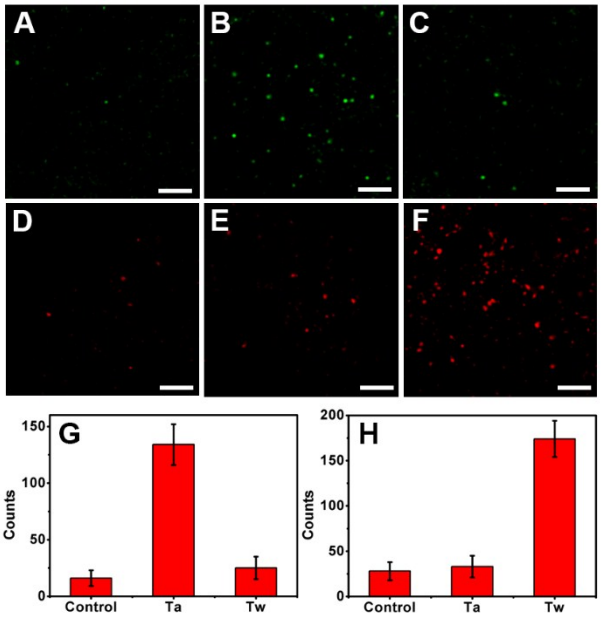


**Fig. S11** Single-nucleotide mutation identification assays by TIRF-based single-molecule imaging. A fluorescence image of PA (A) in the absence of targets (control), (B) in the presence of Ta, and (C) in the presence of Tw. A fluorescence image of PW (D) in the absence of targets (control), (E) in the presence of Ta, and (F) in the presence of Tw. Ta and Tw are the sequences of KRAS G12D (c.35G>A) mutation and wild-type. Measurement of the (G) FG-AgNCs counts in the PA sensing platform, corresponding to (A)-(C) and (H) FR-AgNCs counts in the PW sensing platform, corresponding to (D)-(F). The concentration of targets was 2 nM. Error bars represent the standard deviations of the three experiments and the scale bar is 5 μm.

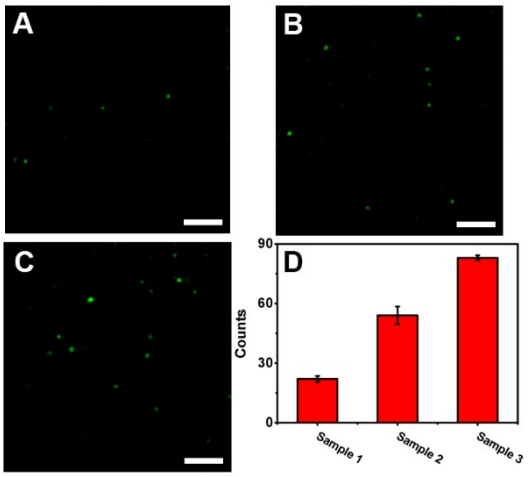


**Fig. S12** Recovery tests for miR-21-spiked human serum samples. Fluorescence images of FG-AgNCs obtained by TIRF-based single-molecule imaging in the presence of miR-21 with different concentrations: (A) 50 pM, (B) 250 pM, (C) 500 pM. The scale bar is 5 mm. (D) Measurement of FG-AgNCs counts in response to the miR-21-spiked human serum samples. Sample 1, 2 and 3 are the serum samples spiked with 50 pM, 250 pM and 500 pM miR-21, respectively. The error bars represent the standard deviations of the three experiments.